Carbohydrate Polymers 92 (2013) 1586–1595

Contents lists available at SciVerse ScienceDirect

Carbohydrate Polymers

journal homepage: www.elsevier.com/locate/carbpol

Mannose-poly(ethylene glycol)-linked SPION targeted to antigen presenting cells for magnetic resonance imaging on lymph node

Muthunarayanan Muthiah[a,b,1], Hieu Vu-Quang[a,b,1], You-Kyoung Kim[c], Joon Haeng Rhee[b], Sang Hyeon Kang[d], Soo Youn Jun[d], Yun-Jaie Choi[c], Yong Yeon Jeong[e], Chong-Su Cho[c,**], In-Kyu Park[a,b,*]

[a] Department of Biomedical Sciences and Center for Biomedical Human Resources (BK-21 project), Chonnam National University Medical School, Gwangju 501-757, South Korea
[b] Clinical Vaccine R&D Center, Chonnam National University Hwasun Hospital, Jeonnam 519-763, South Korea
[c] Department of Agricultural Biotechnology and Research Institute for Agriculture and Life Sciences, Seoul National University, Seoul 151-921, South Korea
[d] iNtRON Biotechnology, Inc., Seongnam 462-120, South Korea
[e] Department of Radiology, Chonnam National University Hwasun Hospital, Jeonnam 519-763, South Korea

ARTICLE INFO

Article history:
Received 27 September 2012
Received in revised form 3 November 2012
Accepted 4 November 2012
Available online 13 November 2012

Keywords:
Mannose
SPION
Mannose receptor
Antigen-presenting cells
Lymph node
MR imaging

ABSTRACT

The aim of this study is to prepare biocompatible and targetable nanoparticles in lymph nodes (LNs) for lymph node-specific magnetic resonance (MR) imaging. Mannan-coated superparamagnetic iron oxide nanoparticles (SPIONs) (mannan-SPION), carboxylic mannan-coated SPION (CM-SPION), and β-glucan-coated SPION (Glucan-SPION) have been developed to target antigen-presenting cells (APCs), for lymph node detection by MR imaging. In this study, mannose-polyethylene glycol (PEG) was prepared by conjugating D-mannopyranosylphenyl isothiocyanate and amine-PEG-carboxyl. The 3-aminopropyltriethoxysilane (APTES)-activated SPION and the mannose-PEG were cross-linked to produce mannose-PEG-linked SPION (Mannose-PEG-SPION). Mannose-PEG-SPION carrying mannose on the surface were assumed efficient at targeting APCs through the specific interactions of the mannose tethered on the Mannose-PEG-SPION and the mannose receptors on the antigen presenting cells. The hydrophilic PEG corona layer in the Mannose-PEG-SPION could be prevented from aggregation during the systemic circulation with accompanying enhanced specificity and minimized systemic toxicity. The accumulation of SPION in the lymph nodes led to increased negative enhancement in the MR images. In the *in vivo* study, rats were injected intravenously with Mannose-PEG-SPION and PEG-SPION, as a control and then tracked by MR imaging after 1 h, 2 h, 3 h, and 24 h. MR imaging on lymph nodes clearly revealed the preferential uptake of Mannose-PEG-SPION in immune cell-rich lymph nodes. The predominant accumulation of Mannose-PEG-SPION in the lymph nodes was also confirmed by Prussian blue staining. Based on these results, Mannose-PEG-SPION shows great potential for lymph node-specific MR imaging.

1. Introduction

Targeted delivery to the site of action has clear therapeutic advantages because it maximizes therapeutic efficiency and minimizes systemic toxicity (Vyas, Singh, & Sihorkar, 2001). Other advantages of targeted delivery are simplified administration and reduced amount of therapeutic molecules required for successful therapy. However, the main advantage is that the local concentration of the therapeutic molecules is elevated, thus protecting the normal cells in cases of cancer and providing more safety and biocompatibility. Considering the immunogenicity of antibodies, carbohydrates were explored for targeted drug or gene delivery and imaging. Specific interactions of carbohydrates with endogenous lectins showed a large number of carbohydrate-binding proteins expressed on mammalian cell surfaces (Yamazaki et al., 2000). Increased expression of lectins was confirmed in malignant cells that are believed to be involved in cancer metastasis, and thus are potential targets for the delivery of drug, gene, or imaging agents to malignant cells (Gabius, 2004). Lectins were investigated as potential targeting moieties for cell surface carbohydrates. Macrophages express carbohydrate receptors, such as the macrophage–mannose receptor, to recognize invaded pathogens. Mannose receptors were expressed abundantly in the immune cells, such as Kupffer cells in

* Corresponding author at: Department of Biomedical Sciences, Chonnam National University Medical School, 5, Hak-1-dong, Gwangju 501-746, South Korea. Tel.: +82 61 379 8481; fax: +82 61 379 8455.
** Corresponding author. Tel.: +82 2 880 4868; fax: +82 2 875 2494.
E-mail addresses: chocs@snu.ac.kr (C.-S. Cho), pik96@chonnam.ac.kr, pik96d@gmail.com (I.-K. Park).
[1] These two authors have contributed to this work equally.

0144-8617/$ – see front matter © 2012 Elsevier Ltd. All rights reserved.
http://dx.doi.org/10.1016/j.carbpol.2012.11.011

the liver, sinusoidal lining cells in the spleen, alveolar macrophages, macrophages in the lymph nodes, and immune cells near the tumor microenvironment. The inclusion of specific ligands on the surface of nanoparticles was shown to enhance significantly the rates and extent of uptake by immune cells such as APCs (Jiang et al., 2009; Kim, Jin, Kim, Cho, & Cho, 2006). Macrophages accumulate at pathological sites, including infection, tumors, atherosclerotic plaques, and arthritic joints and are an important target for drug delivery, gene delivery, and tissue-specific imaging. In our previous study, we demonstrated that mannan-coated SPION (mannan-SPION) was specific to immune cells in LN because of mannose receptor-mediated endocytosis, facilitation of preferential uptake in APCs, faster acquisition, and an enhanced contrast of the MR imaging in target tissues, as compared with Dextran-coated SPION (Dex-SPION) and PVA-coated SPION (PVA-SPION) (Hieu et al., 2011). It was also previously reported by our group that SPION coated with β-glucan could target APCs because glucan was reported to elicit immune responses through the activation of macrophages by an immune cell-specific (1, 3)-β-D-glucan receptor or dectin-1 receptor. β-Glucan-coated SPION was internalized by the immune cells residing in the metastatic liver, which aided in discrimination between metastasized tumor regions and normal hepatic parenchymal tissue. β-Glucan also induces the immune system, which aids in anti-tumor activity (Vu-Quang, Muthiah, Lee, et al., 2012). However, the mannose component of the *Candida albicans* cell wall was identified as a stimulus for tumor necrosis factor alpha (TNFa) secretion (Ataoglu, Dogan, Mustafa, & Akarsu, 2000). It is known that TNFa is among the cytokines that have endogenous pyrogenic activity. The pyrogenic effects of systemically injected yeast mannoses that originated from *C. albicans* and *Saccharomyces cerevisiae* were previously reported in rabbits. We hypothesized that the conjugation of mannose on the surface of iron oxide nanoparticles with PEG linker might reduce this undesired toxic response. This hypothesis is based on the fact that PEGylation has many advantages, such as prolonged residence in the body, decreased degradation by metabolic enzymes, and reduction or elimination of protein immunogenicity (Yuan, Fabregat, Yoshimoto, & Nagasaki, 2011). It was demonstrated that PEGylation is a useful strategy to minimize the biofouling and aggregation of SPION in physiological conditions because of its hydrophilicity and steric repulsion of PEG chains (Islam et al., 2010; Liu et al., 2011).

In this work, we synthesized mannose-PEG-linked SPION (Mannose-PEG-SPION) for targeting to APCs through the specific interactions of mannose on the SPION with mannose receptor on APCs in the lymph node, which can be tracked by MR imaging. The presence of Mannose-PEG-SPION in lymph nodes was also confirmed by histological analysis.

2. Materials and methods

NH2-PEG-COOH (Mw 2 kDa) was purchased from NOF Corporation, USA. D-Mannopyranosylphenyl isothiocyanate, ferric chloride hexahydrate ($FeCl_3 \cdot 6H_2O > 97\%$), and ferrous chloride tetrahydrate ($FeCl_2 \cdot 4H_2O > 99\%$) were purchased from Sigma–Aldrich (St. Louis, MO, USA). All other chemicals were of analytical reagent grade and were used without further purification.

2.1. Synthesis and characterization of mannose-PEG-COOH and Mannose-PEG-SPION

Mannose-PEG-COOH was prepared without reagents from the direct conjugation of NH_2-PEG-COOH (2 kDa) and D-mannopyranosylphenyl isothiocyanate. Both chemicals were dissolved in dimethylsulfoxide (DMSO) and agitated at 25 °C for 24 h. The SPION was synthesized by a modified co-precipitation method, in accordance with a previous study (Yoo et al., 2008). Following the addition of NH_4OH, SPION was prepared by an alkaline co-precipitation of $FeCl_3 \cdot 6H_2O$ and $FeCl_2 \cdot 4H_2O$ with a Fe(III)/Fe(II) feed ratio of 3:1 in deoxygenated water. The black precipitate was washed several times, and the final pH was adjusted from 10 to 7. The solution was allowed to sediment under a magnetic field, and the supernatant was discarded. The black sediment was mixed with 2 M HNO_3 and 0.35 M $Fe(NO_3)_3$. The suspension was dialyzed for 2 days against 0.01 M HNO_3 and stored at 4 °C. The prepared SPION was mixed with 3-aminopropyltriethoxysilane (APTES) and dissolved in ethanol under a nitrogen atmosphere for 24 h to produce APTES-activated SPION (APTES-SPION). APTES-SPION were then conjugated to an excess amount of mannose-PEG-COOH (10 times by weight) with an EDC/NHS coupling agent at 25 °C for 24 h. The amount of PEG conjugated to SPION was optimized by thermogravimetric analysis. The synthesized mannose-PEG-COOH was analyzed by ^1H nuclear magnetic resonance spectroscopy (^1H NMR, Avance_600, Bruker, Germany). The Fourier transform infrared (FT-IR) spectra were measured using a Nicolet Magna 550 series II (Midac, Atlanta, GA, USA). The particle sizes of the Mannose-PEG-SPION were assessed using an electrophoretic light-scattering spectrophotometer (ELS 8000, Otsuka Electronics, Osaka, Japan), with 90° and 20° scattering angles at 25 °C. An electrophoretic mobility measurement was performed using the same setting equipped with a platinum electrode. The morphology of Mannose-PEG-SPION was also obtained by using a JEOL JEM-1010 transmission electron microscope (TEM).

2.2. Primary peritoneal macrophage isolation

Peritoneal macrophages were isolated as reported in our previous study (Vu-Quang, Muthiah, Kim, et al., 2012). In brief, 3 ml of Brewer thioglycollate medium (Fluka, Mumbai, India) was injected first into the peritoneal cavity of inbred Balb/c mice (7 weeks, male) (Orient Bio Inc., Seongnam-si, South Korea). 3 days after injection of Brewer thioglycollate medium, ice cold RPMI 1640 (Thermo Scientific, Logan, UT) was injected into the peritoneal cavity, in order to suspend the enriched peritoneal macrophages. The fluid was withdrawn, washed with PBS, and centrifuged three times at 1000 r.p.m. for 10 min. Macrophages were allowed to adhere to the cell culture dish in serum-free RPMI 1640 for 2 h at 37 °C and 5% CO_2. The cells were washed with cold PBS three times and the adherent cells harvested using a cell scraper.

2.3. Cytotoxicity of Mannose-PEG-SPION

Isolated peritoneal macrophages were seeded in 96 well plates at a density of 2×10^4/well in 100 μL of RPMI 1640 growth medium and incubated overnight at 37 °C in 5% CO_2. The cells were treated with Mannose-PEG-SPION, PEG-linked SPION (PEG-SPION), and SPION at various concentrations (50–500 μg Fe/ml) for 24 h. The cells were then incubated with 100 μL of 3-(4,5-dimethylthiazol-2-yl)-2,5-diphenyltetrazolium bromide (MTT) solution for 4 h to allow the formation of formazan crystals by mitochondrial dehydrogenases. The medium was removed, and 100 μL of DMSO was added to dissolve the formazan crystals. The optical density of the solution was measured at a wavelength of 570 nm, using a Spectra Max 190 spectrophotometer (Molecular Devices, Sunnyvale, CA).

2.4. Systemic toxicity of Mannose-PEG-SPION

A toxicological comparison was performed between Mannose-PEG-SPION and mannan-SPION, using the conventional single-dose intravenous toxicity test. The test was performed at the Korea Institute of Toxicology, Korea Research Institute of Chemical

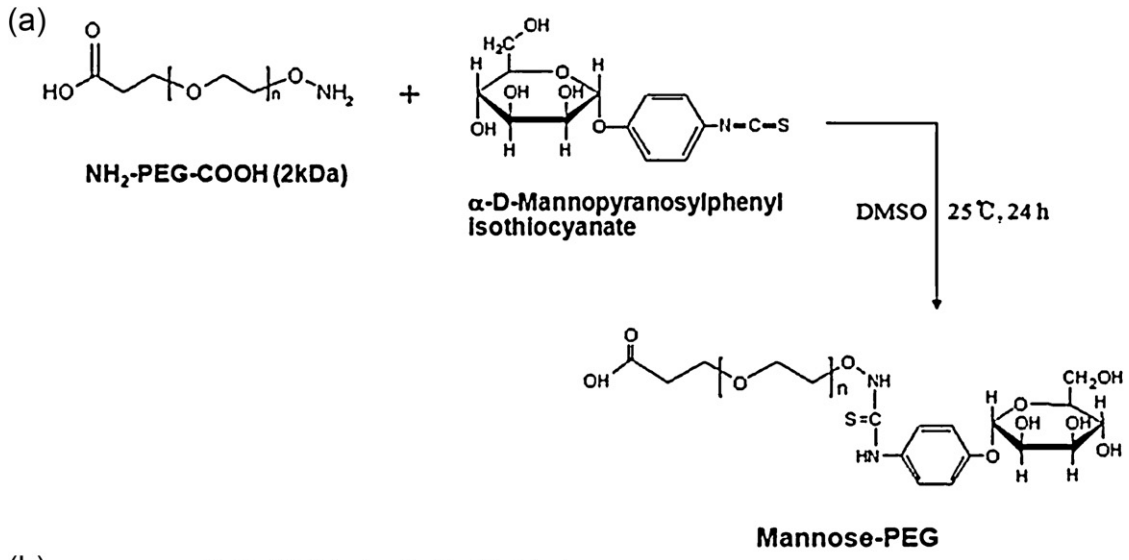

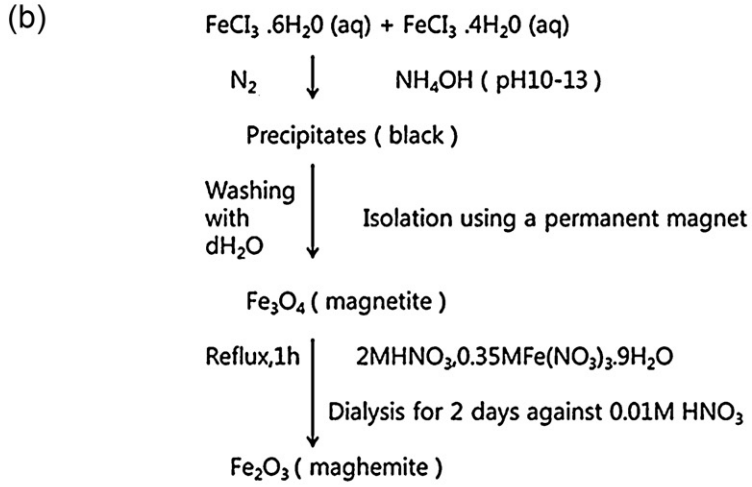

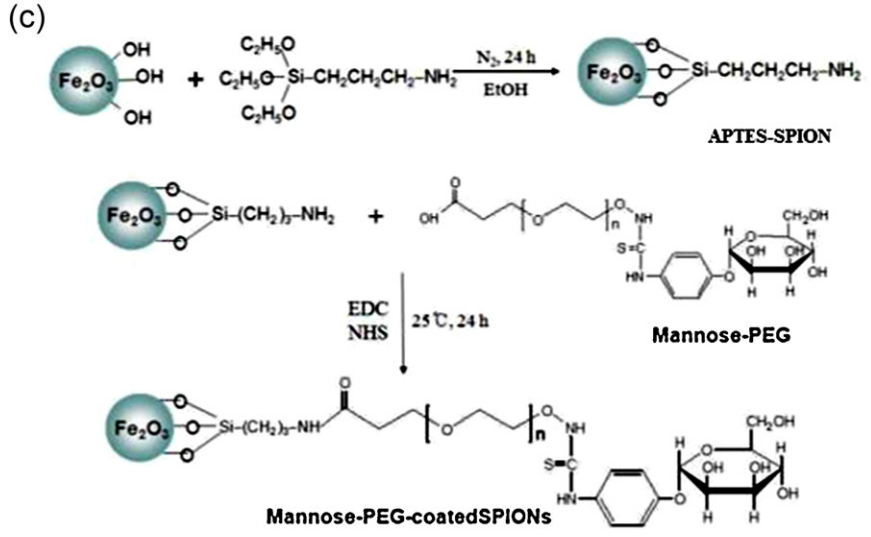

Scheme 1. (a) The synthesis scheme of mannose-PEG-COOH, (b) co-precipitation procedure to prepare SPION. (c) The conjugation of mannose-PEH-COOH with APTES-SPION to produce Mannose-PEG-SPION.

Technology. Either Mannose-PEG-SPION or mannan-SPION was administered by intravenous injection to 7-week-old ICR mice (five male mice and five female mice per group) at different doses of 0, 20, and 40 mg Fe/kg. General symptoms, deaths, and weight changes in mice were observed for 15 days. All abnormal signs in the internal organs were checked by autopsy. All experiments were performed after approval by the local ethics committee at Chonnam National University Medical School (CNU IACUC-H-2011-5) and are in accordance with the principles of laboratory animal care (NIH publication #85-23).

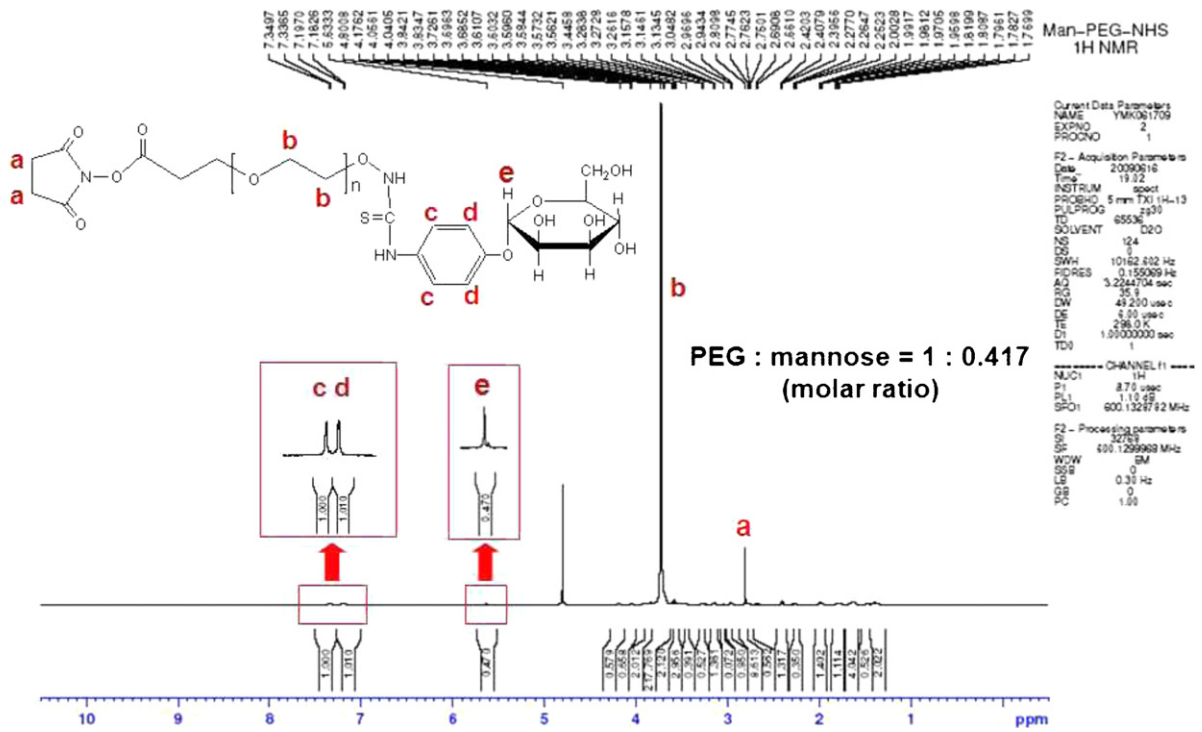

Fig. 1. The confirmation of conjugation between mannose isothiocyanate and bifunctional PEG (NH_2-PEG-COOH) by a ^{1}H-NMR analysis.

2.5. *In vivo* MR imaging on lymph nodes with Mannose-PEG-SPION

In the case of the *in vivo* MRI study, SPF/VAF-outbred rats (7 week old males) (Orient, Seongnam, Korea) were pre-scanned using clinical MR IMAGING equipment (Siemens wrist coil for rats and Siemens volume coil for mice) in the LN area. All experiments were performed after approval by the local ethics committee at Chonnam National University Medical School and are in accordance with the principles of laboratory animal care (NIH publication #85-23). MR imaging was used to assess the accumulation of Mannose-PEG-SPION and PEG-linked SPION in the LNs. The scanning protocol included the acquisition of T2-weighted spin-echo coronal images used for the localization of LN (measured parameters: slice thickness 1 mm, matrix 256 × 218, TR = 3000 ms, NEX = 2, TE = 104 ms, 1 average, FOV 100 mm × 100 mm, and flip angle = 150°). Immediately after pre-scanning, Mannose-PEG-SPION of 12.5 mg Fe/kg (five rats in each group) was injected into the rats, which were scanned after 1, 2, 3, and 24 h in the same locations. The rats were sacrificed after the last scan. Signal intensities from the muscle region and the LN were measured and converted to the relative intensity ratio between the LN and the muscle. The signal intensity ratio from the pre-scanning imaging was set at 100%.

2.6. Histological analysis with Prussian blue staining

Paraffin blocks were prepared from the fixed peritoneal macrophages and tissue samples and processed for Prussian blue staining. Each paraffin-embedded sample was sliced into 5 μm sections, which were placed on glass slides. The sections were deparaffinized and serially hydrated by immersing the slides twice in 100% xylene, twice in 100% ethanol, and once in 95%, 90%, 80%, and 70% ethanol. The hydrated slides were washed under tap water for 5 min and stained with a 1:1 mixture of 20% HCl and 10% potassium ferrocyanide trihydrate for 20 min. The slides were then counterstained with a nuclear fast red solution (Sigma–Aldrich) for 5 min. The stained slide was mounted in a Permount™ solution (Fisher Scientific, PA, USA).

3. Results and discussion

Mannose is a component found on the surface of microorganisms. Mannose residues are recognized by mannose-binding lectins (complement system) and mannose receptors on APCs (Vu-Quang, Muthiah, Kim, et al., 2012). After the mannose is bound to the mannose receptors on the APC, it is phagocytosed by immune cells in the local immune system, such as LN. In our previous study, we observed the following characteristics of mannose-SPION: (1) efficient for targeting APC; (2) faster and enhanced accumulation in LN; and (3) detects metastatic LN. The preferential and faster uptake of mannan-SPION over PVA and Dex-SPION was demonstrated by Prussian blue staining, MR imaging *in vitro* phantom tube imaging, and their distribution *in vivo*, confirming the accumulation of lymph nodes in the liver and the kidneys (Hieu et al., 2011). The focus of this study is to improve the biocompatibility and specificity of mannose SPION, which will also help to increase the circulation time.

3.1. Synthesis of mannose-PEG and Mannose-PEG-SPION

D-Mannopyranosylphenyl isothiocyanate reacts with the nucleophile amine from NH_2-PEG-COOH, and the reaction involves the attack of a nucleophile on the central electrophilic carbon of the isothiocyanate group. The resulting electron shift and proton loss creates a thiourea linkage between the D-mannopyranosylphenyl isothiocyanate and NH_2-PEG-COOH (Scheme 1(a)). The chemical composition of synthesized mannose-PEG-COOH was confirmed by ^{1}H NMR analysis (Fig. 1). The characteristic peaks occurring at 3.64 ppm in the ^{1}H NMR spectrum were due to the resonance of methylene protons in PEG (—OCH_2CH_2—). The 5.63 ppm is the characteristic peak representing the mannose after conjugation with PEG. The reaction yield was found to be 41.7 mol% after the conjugation.

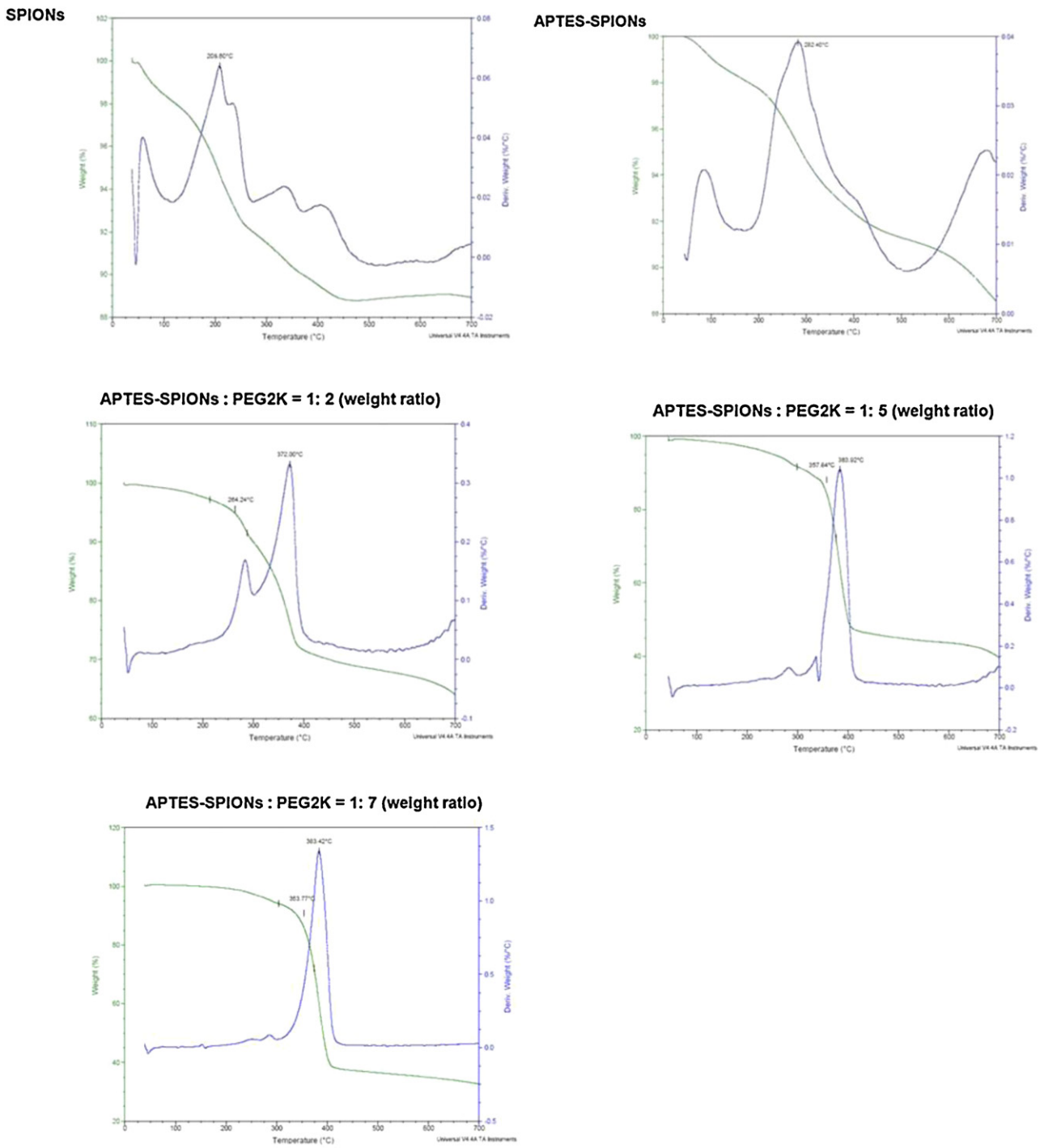

Fig. 2. Optimization of the conjugation ratio of SPION to PEG, estimated by a thermogravimetric analysis. PEG-SPION synthesized with different conjugation ratios were analyzed by thermogravimetric analysis.

SPION were prepared by co-precipitation, as mentioned in Scheme 1(b). The prepared SPION was activated with APTES to allow for amine functionality on the surface of the SPION, which was utilized for further modification. Mannose-PEG-SPION were synthesized by EDC/NHS crosslinking. The amine group from the APTES-SPION and the carboxyl group from the mannose-PEG-COOH were linked to form the amide bond through EDC/NHS coupling (Scheme 1(c)). The TGA analysis of PEG-SPION with various SPION:PEG weight ratios of 1:2, 1:3, 1:5, and 1:7 were performed to determine the optimal conjugation ratio. The results showed that the amount of PEG content in the PEG-SPION increased steadily when the weight ratio of SPION to PEG reached 1:5, whereas the PEG amount did not increase much after the weight ratio reached 1:7. When PEG-SPION was synthesized at the weight ratio of 1:5, the major mass loss was approximately 36%, which occurred between 200 and 450 °C, and could be ascribed to the pyrolysis of PEG on the surface of PEG-SPION (Fig. 2). The FT-IR spectrum of PEG-SPION exhibited peaks around 1541 and 1647 cm^{-1}, which were assigned to the amide carbonyl groups and N–H bending, respectively, and indicated the successful linkage of amino groups in PEG to the surface of APTES-activated SPION *via* amidation reaction. Additionally, IR absorption at 1145 cm^{-1} and

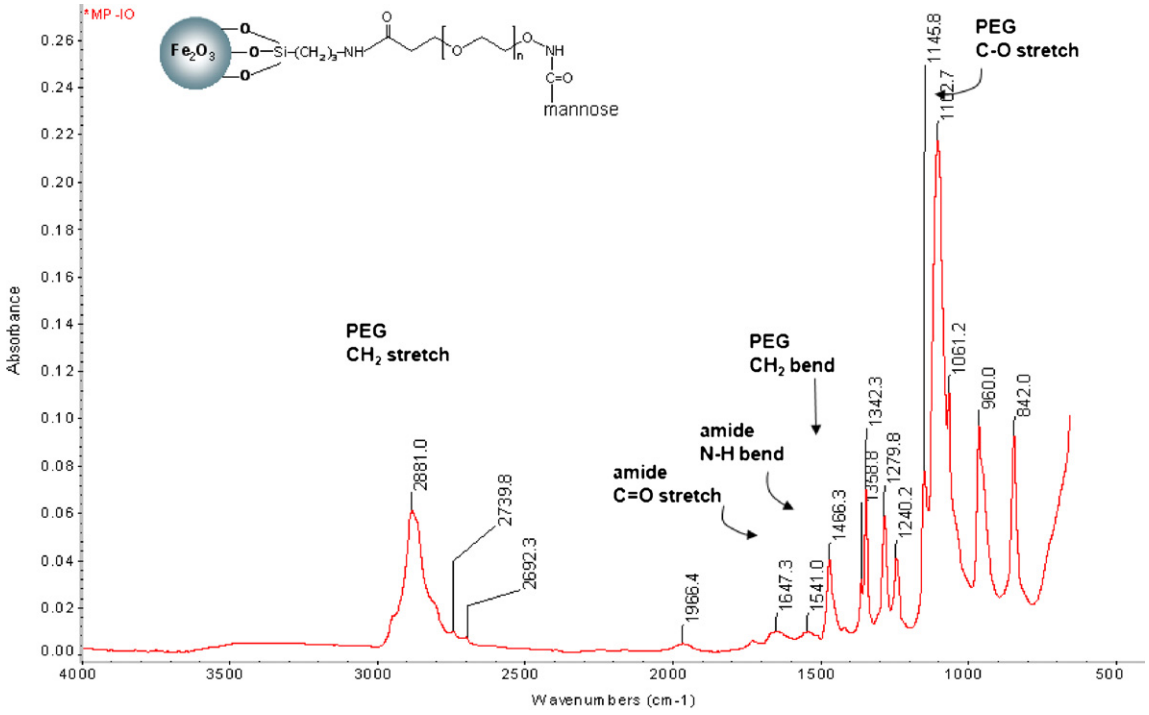

Fig. 3. The chemical confirmation of synthesized Mannose-PEG-SPION was measured by FT-IR.

2881 cm^{-1} also corresponds to the C–O and CH_2 stretching peaks of PEG, respectively. Accordingly, the results of FT-IR explicitly demonstrate the formation of Mannose-PEG-SPION (Fig. 3).

3.2. Characterization of Mannose-PEG-SPION

The hydrodynamic size of Mannose-PEG-SPION in an aqueous medium was measured by dynamic light scattering (DLS) at around 22.2 ± 5.4 nm. The TEM image indicates that Mannose-PEG-SPION was well separated and slightly ellipsoidal in shape. The DLS-based average particle sizes with Mannose-PEG-SPION were larger than the sizes measured by TEM observation, because of the hydrodynamic volume of mannose-PEG occupied in aqueous solution. The aqueous stability of the particles was also measured for a period of 4 weeks. The particles remained stable in the aqueous solution, and the average size of the Mannose-PEG-SPION did not vary during that period, confirming the aqueous stability and non-aggregation. The surface charge of Mannose-PEG-SPION was also measured by a zeta potential analysis, which was approximately +20 mV (Figs. 4 and 5). The presence of a positive charge on Mannose-PEG-SPION after PEGylation may be caused by the unreacted amino groups on the surface of APTES-SPION and PEG. The positive charge helps in electrostatic repulsion, resulting in non-aggregation (Lee, Nguyen, et al., 2012; Lee, Muthiah, et al., 2012).

3.3. Cytotoxicity of Mannose-PEG-SPION

Mannose-PEG-SPION, PEG-SPION, and SPION at various concentrations were treated with murine peritoneal macrophage cells, and the cellular viability after the treatment with those SPION was analyzed by MTT assay. Fig. 6 shows the MTT assay results for the cytotoxicity of the SPION against murine peritoneal macrophage cells that were isolated from the murine peritoneal cavity. The cell viability of the Mannose-PEG-SPION-treated group was not affected by the treated ferric ion concentration, which ranged from 30 to 500 μg, indicating that Mannose-PEG-SPION displayed no cytotoxicity. PEG-SPION exhibited cytotoxicity similar to Mannose-PEG-SPION, probably because of the surface shielding effect of the PEG corona (Lee et al., 2005). In case of an unmodified SPION, the cellular toxicity was raised to 50% when 500 μg of ferric ion was treated, indicating a higher toxicity than that of the biocompatible Mannose-PEG-SPION (Fig. 6). Thus, Mannose-PEG-SPION appears to be a useful nontoxic contrast agent for MR imaging.

3.4. Systemic toxicity of CM-SPION

Mannose-PEG-SPION or mannan-SPION was administered in doses of 20, 40, and 80 mg Fe/kg by intravenous injection to 7-week-old ICR mice (five male mice and five female mice per group). The mice administered with more than 20 mg Fe/kg of mannan-SPION either died or showed specific symptoms of subdued behavior, irregular respiration, prone position, and lower abdomen contamination. A 50% lethal dose (LD_{50}) of mannan-SPION was determined to be 20 mg Fe/kg in both male and female mice (Table 1). On the other hand, the mice administered with Mannose-PEG-SPION showed no abnormality; both male and female mice remained healthy during the observation period. The LD_{50} of Mannose-PEG-SPION was much higher than 40 mg Fe/kg in the mice (Table 1). This result indicates that Mannose-PEG-SPION appears to be a biocompatible MR imaging contrast agent with an improved biosafety profile compared to that of mannan-SPION.

Table 1
The systemic toxicity of mannan-SPION and Mannose-PEG-SPION was observed after administering doses of 0, 20, and 40 Fe/kg by intravenous injection to 7-week-old ICR mice. Systemic toxicity was expressed as an LD_{50} value in mg/kg.

	LD_{50} (mg/kg)
Mannan-SPION	20
Mannose-PEG-SPION	≫40

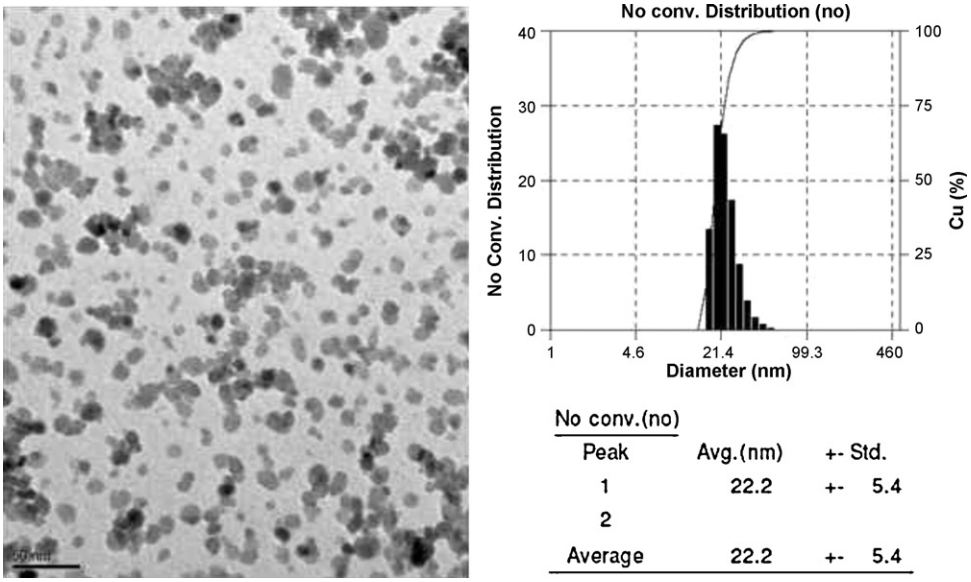

Fig. 4. The morphology and hydrodynamic size distribution of Mannose-PEG-SPION was measured by a transmission electron microscopy and dynamic light scattering, respectively.

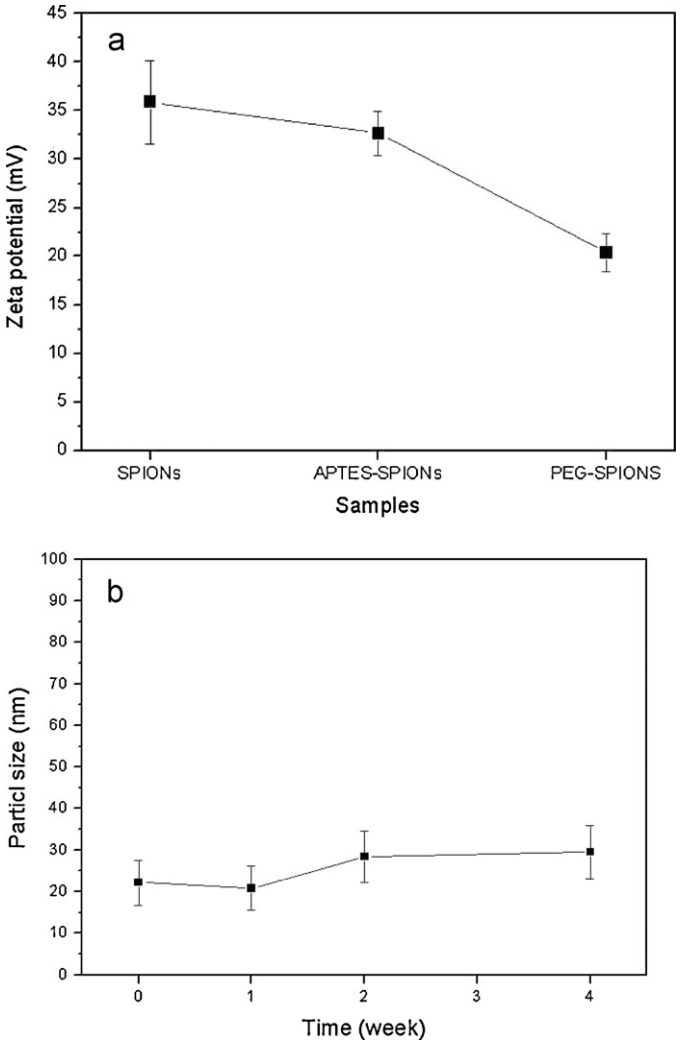

Fig. 5. A reduction in the surface charge of PEG-SPION was measured by a zeta potential analysis (a). The aqueous stability of Mannose-PEG-SPION in a medium was determined by the measurements of the particle size over a period of time (b).

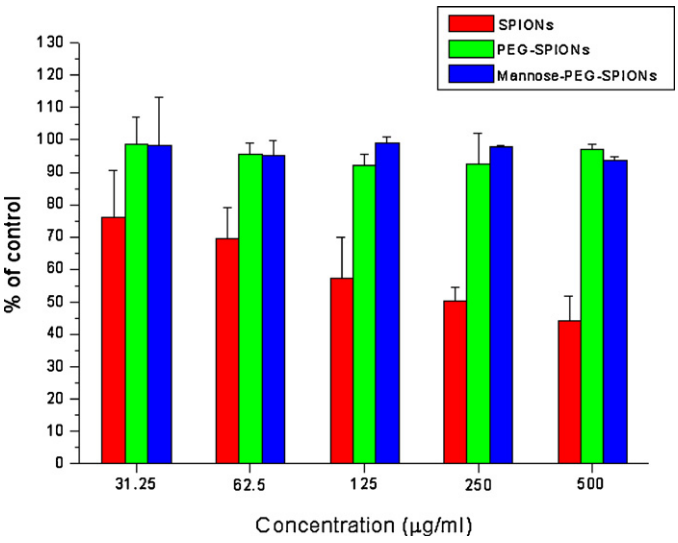

Fig. 6. The cellular viability of murine peritoneal macrophages against Mannose-PEG-SPION, PEG-SPION, and unmodified SPION at 24 h after incubation, measured by a MTT assay.

3.5. In vivo MR imaging on lymph nodes with Mannose-PEG-SPION

MR imaging of the rat's lymph nodes was performed 24 h after the intravenous injection of Mannose-PEG-SPION and PEG-SPION. When conducting MR imaging, T2-weighted gradient echo imaging is a useful option to evaluate the accumulation of SPION *in vivo*. Normal rats were used to investigate the macrophage targeting ability of Mannose-PEG-SPION as an MR imaging contrast agent. The T2-weighted MR images of the rats after the intravenous injection of Mannose-PEG-SPION and PEG-SPION are shown in Fig. 7. The signal intensity of the LN on T_2-weighted MR Is after the injection of the contrast agent was negatively enhanced compared to that of the T2-weighted MR images of the same LN before the injection. In the presence of SPION, the signal in the T2-weighted sequence became darker (negative enhancement), which was caused by the shortening of the proton spin. The Mannose-PEG-SPION was accumulated

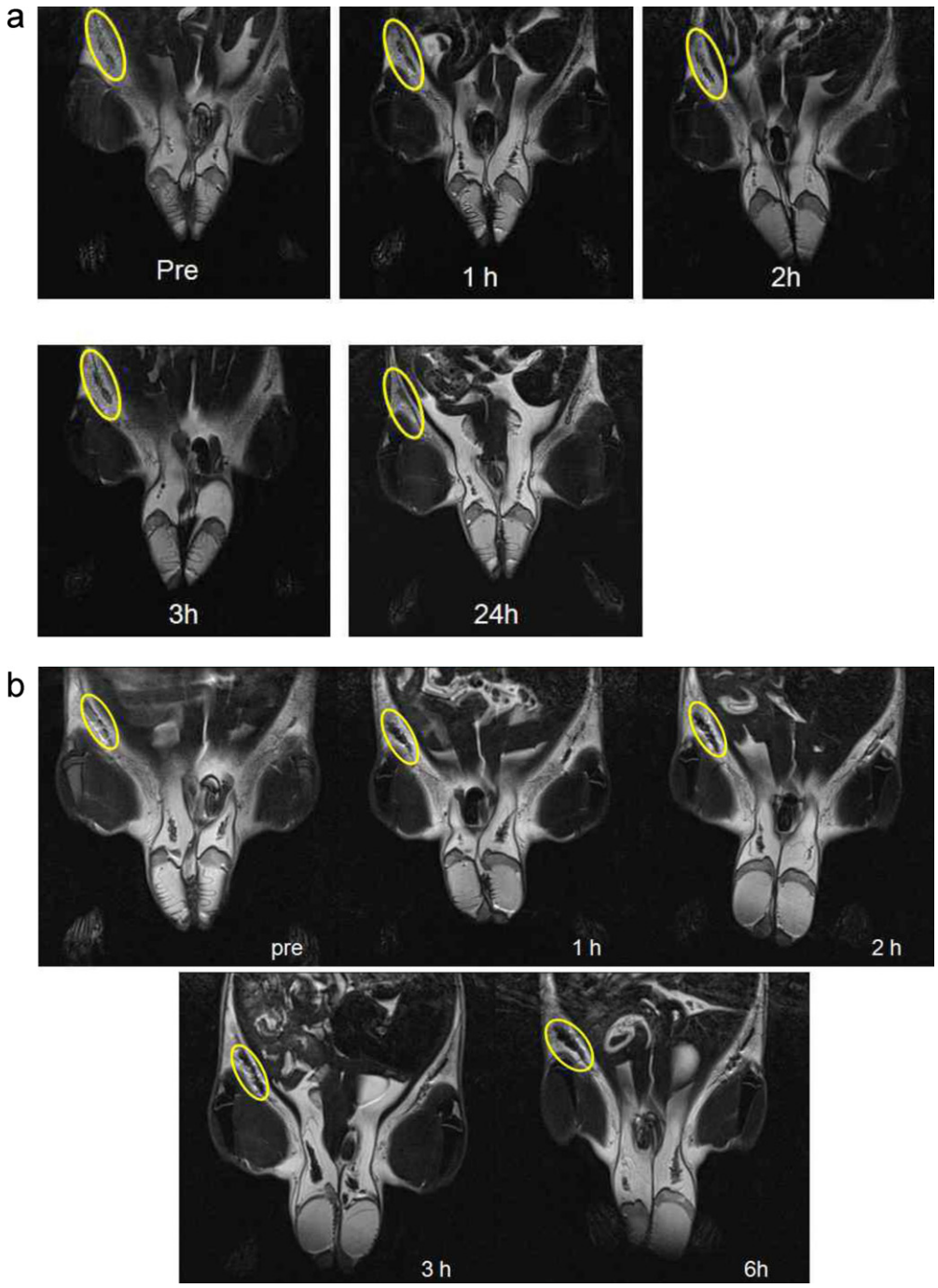

Fig. 7. The time-dependent accumulation of PEG-linked SPION (a) and Mannose-PEG-SPION (b) in lymph nodes after an intravenous injection, measured by MR imaging.

mainly in the LN after the intravenous injection. The accumulation of Mannose-PEG-SPION and PEG-linked SPION in the LN was also confirmed by Prussian blue staining, as shown in Fig. 8. The blue dots indicate the presence of iron inside the immune cells of the lymph nodes and the pink represents the nucleus.

It was previously reported that LN could be detected by MR imaging at 24 h after the administration of ferumoxtran-10 (AMI-227), a type of Dextran-coated SPION (Detre et al., 1999; Harisinghani et al., 2003; Raty et al., 2007). The accumulation of SPION at LN follows two potential pathways: (1) direct accumulation in the circulating APC, followed by migration to the LN; (2) migration of the contrast agent *via* lymphatic vessels to the draining LN from the systemic circulation (Hamm, 2002; Weissleder, Bogdanov, Neuwelt, & Papisov, 1995; Yoo et al., 2012). In the results of our study, we observed a negative enhancement in the LN region with Mannose-PEG-SPION 1 h post-injection, which was significantly different from the intensities in LN with the PEG-SPION injected group. Furthermore, it seemed that the presence of a higher number of mannose receptor-positive APCs in the LN also promoted a faster accumulation of Mannose-PEG-SPION. The MR signal intensity of the LN with Mannose-PEG-SPION remained stable up to 24 h after the systemic injection. From the histological analysis, it is evident that the LN accumulation of Mannose-PEG-SPION is more enhanced than that of PEG-SPION. A uniform and dense distribution of Mannose-PEG-SPION accumulated in the LN compared to the PEG-SPION. The dense distribution might help in the prominent MR imaging of lymph nodes. Our results for *in vivo* accumulation in LN, which were measured by MR imaging and Prussian

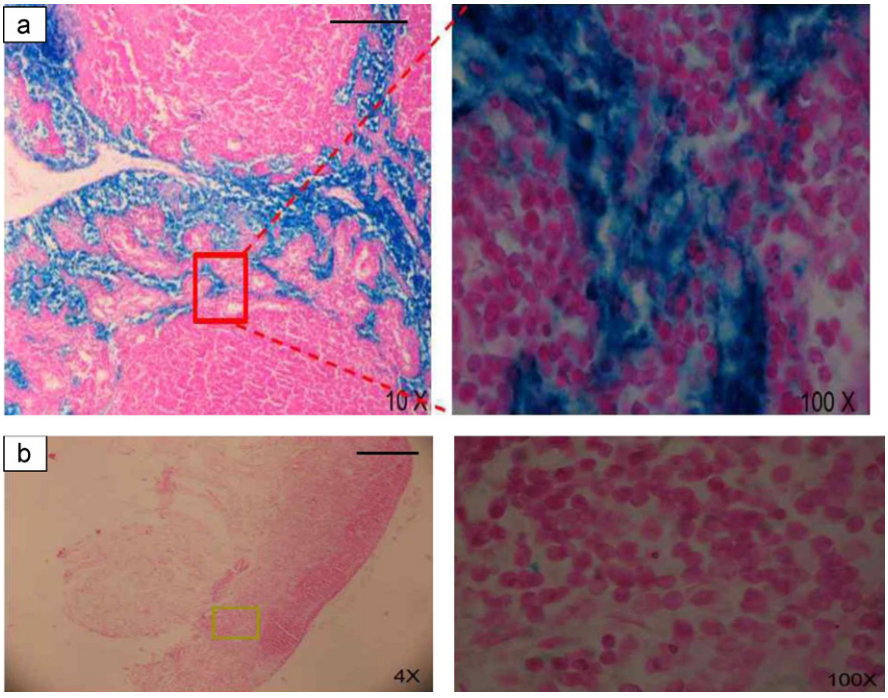

Fig. 8. Prussian blue staining on lymph nodes at 24 h after the intravenous injection of Mannose-PEG-SPION (a) and PEG-SPION (b). 500 μL (Fe 0.265 mg) of each sample was injected intravenously and rats were sacrificed at 24 h after the injection. The LN was sectioned and stained by a Prussian blue stain. The blue represents iron and the pink represents the nucleus. The scale bar in the figure represents a range of 500 μm.

blue staining, clearly confirmed our theory that the specific binding of Mannose-PEG-SPIONs to APC would enhance the local uptake in LN through a facilitated interaction with APC. Based on these data, we proved that Mannose-PEG-SPION possesses higher specificity toward APCs and are more biocompatible than previously studied mannan-based contrast agents are.

Acknowledgements

This work was financially supported by the Bio Imaging Research Center at GIST. IKP also acknowledges the financial support of the Regional Technology Innovation Program of the Ministry of Commerce, Industry and Energy (Grant RT104-01-01); the Basic Science Research Program through the National Research Foundation of Korea, funded by the Ministry of Education, Science and Technology (2010-0002940); the Small and Medium Business Administration of Korea, the Korea Healthcare Technology R&D Project, Ministry for Health, Welfare & Family Affairs, Republic of Korea (A084869 and A100553); and the Leading Foreign Research Institute Recruitment Program through the National Research Foundation of Korea (NRF), funded by the Ministry of Education, Science and Technology (MEST) (2011-0030034).

References

Ataoglu, H., Dogan, M. D., Mustafa, F., & Akarsu, E. S. (2000). *Candida albicans* and *Saccharomyces cerevisiae* cell wall mannans produce fever in rats—Role of nitric oxide and cytokines. *Life Sciences*, *67*(18), 2247–2256.

Detre, J. A., Samuels, O. B., Alsop, D. C., Gonzalez-At, J. B., Kasner, S. E., & Raps, E. C. (1999). Noninvasive magnetic resonance imaging evaluation of cerebral blood flow with acetazolamide challenge in patients with cerebrovascular stenosis. *Journal of Magnetic Resonance Imaging*, *10*(5), 870–875.

Gabius, H. J. (2004). The sugar code in drug delivery. *Advanced Drug Delivery Reviews*, *56*(4), 421–424.

Hamm, B. (2002). Iron-oxide-enhanced MR lymphography: Just a new toy or a breakthrough? *European Radiology*, *12*(5), 957–958.

Harisinghani, M. G., Barentsz, J., Hahn, P. F., Deserno, W. M., Tabatabaei, S., van de Kaa, C. H., et al. (2003). Noninvasive detection of clinically occult lymph-node metastases in prostate cancer. *New England Journal of Medicine*, *348*(25), 2491–2499.

Hieu, V. Q., Yoo, M. K., Jeong, H. J., Lee, H. J., Muthiah, M., Rhee, J. H., et al. (2011). Targeted delivery of mannan-coated superparamagnetic iron oxide nanoparticles to antigen-presenting cells for magnetic resonance-based diagnosis of metastatic lymph nodes in vivo. *Acta Biomaterialia*, *7*(11), 3935–3945.

Islam, M., Yoo, M. K., Lim, H. T., Jiang, H. L., Lee, S. J., Park, I. K., et al. (2010). Folate-Peg-Superparamagnetic iron oxide nanoparticles labeled with Cy5.5 for lung cancer imaging. *Atherosclerosis Supplements*, *8*(8), 3005–3013.

Jiang, H. L., Kim, Y. K., Arote, R., Jere, D., Quan, J. S., Yu, J. H., et al. (2009). Mannosylated chitosan-graft-polyethylenimine as a gene carrier for Raw 264.7 cell targeting. *International Journal of Pharmaceutics*, *375*(1–2), 133–139.

Kim, T. H., Jin, H., Kim, H. W., Cho, M. H., & Cho, C. S. (2006). Mannosylated chitosan nanoparticle-based cytokine gene therapy suppressed cancer growth in BALB/c mice bearing CT-26 carcinoma cells. *Molecular Cancer Therapeutics*, *5*(7), 1723–1732.

Lee, C. M., Choi, Y. D., Huh, E. J., Lee, K. Y., Song, H. C., Sun, M. J., et al. (2005). Polyethylene glycol (PEG) modified Tc-99m-HMPAO-liposome for improving blood circulation and biodistribution: The effect of the extent of PEGylation. *Cancer Biotherapy and Radiopharmaceuticals*, *20*(6), 620–628.

Lee, S. J., Muthiah, M., Lee, H. J., Lee, H. J., Moon, M. J., Che, H. L., et al. (2012). Synthesis and characterization of magnetic nanoparticle-embedded multi-functional polymeric micelles for MRI-guided gene delivery. *Macromolecular Research*, *20*(2), 188–196.

Lee, H. J., Nguyen, Y. T. C., Muthiah, M., Vu-Quang, H., Namgung, R., Kim, W. J., et al. (2012). MR traceable delivery of p53 tumor suppressor gene by PEI-functionalized superparamagnetic iron oxide nanoparticles. *Journal of Biomedical Nanotechnology*, *8*(3), 361–371.

Liu, D. F., Wu, W., Ling, J. J., Wen, S., Gu, N., & Zhang, X. Z. (2011). Effective PEGylation of iron oxide nanoparticles for high performance in vivo cancer imaging. *Advanced Functional Materials*, *21*(8), 1498–1504.

Raty, J. K., Liimatainen, T., Kaikkonen, M. U., Grohn, O., Airenne, K. J., & Yla-Herttuala, S. (2007). Non-invasive imaging in gene therapy. *Molecular Therapy*, *15*(9), 1579–1586.

Vu-Quang, H., Muthiah, M., Kim, Y. K., Cho, C. S., Namgung, R., Kim, W. J., et al. (2012). Carboxylic mannan-coated iron oxide nanoparticles targeted to immune cells for lymph node-specific MRI in vivo. *Carbohydrate Polymers*, *88*(2), 780–788.

Vu-Quang, H., Muthiah, M., Lee, H. J., Kim, Y. K., Rhee, J. H., Lee, J. H., et al. (2012). Immune cell-specific delivery of beta-glucan-coated iron oxide nanoparticles for diagnosing liver metastasis by MR imaging. *Carbohydrate Polymers*, *87*(2), 1159–1168.

Vyas, S. P., Singh, A., & Sihorkar, V. (2001). Ligand-receptor-mediated drug delivery: An emerging paradigm in cellular drug targeting. *Critical Reviews in Therapeutic Drug Carrier Systems*, *18*(1), 1–76.

Weissleder, R., Bogdanov, A., Neuwelt, E. A., & Papisov, M. (1995). Long-circulating iron-oxides for MR-imaging. *Advanced Drug Delivery Reviews*, *16*(2–3), 321–334.

Yamazaki, N., Kojima, S., Bovin, N. V., Andre, S., Gabius, S., & Gabius, H. J. (2000). Endogenous lectins as targets for drug delivery. *Advanced Drug Delivery Reviews*, *43*(2–3), 225–244.

Yoo, M. K., Park, I. Y., Kim, I. Y., Park, I. K., Kwon, J. S., Jeong, H. J., et al. (2008). Superparamagnetic iron oxide nanoparticles coated with mannan for macrophage targeting. *Journal of Nanoscience and Nanotechnology*, *8*(10), 5196–5202.

Yoo, M. K., Park, I. K., Lim, H. T., Lee, S. J., Jiang, H. L., Kim, Y. K., et al. (2012). Folate-PEG-superparamagnetic iron oxide nanoparticles for lung cancer imaging. *Acta Biomaterialia*, *8*(8), 3005–3013.

Yuan, X., Fabregat, D., Yoshimoto, K., & Nagasaki, Y. (2011). High PEGylation efficiency of pentaethylenehexamine-end poly(ethylene glycol) (mPEG-N6) for active-ester surface. *Colloids and Surfaces B: Biointerfaces*, *92*, 25–29.